MOLECULAR AND CELLULAR BIOLOGY, June 1997, p. 3103–3115 Vol. 17, No. 6
0270-7306/97/$04.00+0

A Novel Mutant Allele of *Schizosaccharomyces pombe rad26* Defective in Monitoring S-Phase Progression To Prevent Premature Mitosis

MASASHI UCHIYAMA, IVO GALLI, DOMINIC J. F. GRIFFITHS, AND TERESA S.-F. WANG*

Department of Pathology, Stanford University School of Medicine, Stanford, California 94305-5324

Received 23 December 1996/Returned for modification 29 January 1997/Accepted 25 March 1997

A semipermissive growth condition was defined for a *Schizosaccharomyces pombe* strain carrying a thermosensitive allele of DNA polymerase δ (*polδts03*). Under this condition, DNA polymerase δ is semidisabled and causes a delay in S-phase progression. Using a genetic strategy, we have isolated a panel of mutants that enter premature mitosis when DNA replication is incomplete but which are not defective for arrest in G_2/M following DNA damage. We characterized the *aya14* mutant, which enters premature mitosis when S phase is arrested by genetic or chemical means. However, this mutant is sensitive to neither UV nor gamma irradiation. Two genomic clones, *rad26*$^+$ and *cds1*$^+$, were found to suppress the hydroxyurea sensitivity of the *aya14* mutant. Genetic analysis indicates that *aya14* is a novel allele of the cell cycle checkpoint gene *rad26*$^+$, which we have named *rad26.a14*. *cds1*$^+$ is a suppressor which suppresses the S-phase feedback control defect of *rad26.a14* when S phase is inhibited by either hydroxyurea or *cdc22*, but it does not suppress the defect when S phase is arrested by a mutant DNA polymerase. Analyses of *rad26.a14* in a variety of *cdc* mutant backgrounds indicate that strains containing *rad26.a14* bypass S-phase arrest but not G_1 or late S/G_2 arrest. A model of how *Rad26* monitors S-phase progression to maintain the dependency of cell cycle events and coordinates with other *rad/hus* checkpoint gene products in responding to radiation damage is proposed.

Maintaining the genome stability of a cell requires a complex network of checkpoint mechanisms that ensure both that DNA replication cannot be initiated until completion of the previous mitosis and that mitosis does not occur until DNA replication is completed and damaged DNA is repaired (6, 10, 13, 19, 24, 28, 33, 35). Checkpoints that control mitosis in response to DNA status have been investigated genetically in the budding yeast *Saccharomyces cerevisiae* and the fission yeast *Schizosaccharomyces pombe* (1–4, 8, 12, 17, 29, 39, 40, 44–46, 48–50). DNA damage checkpoints respond to radiation damage by delaying cell cycle progression, thereby providing cells time to repair the DNA before entering mitosis (6, 10, 19, 33, 38). When DNA replication is delayed or blocked, the S phase to mitosis checkpoint (hereafter termed the S-M-phase checkpoint or S-phase feedback control) prevents cells from entering mitosis with incompletely replicated chromosomes. Although genetic evidence has indicated that the DNA damage and S-M-phase checkpoint rely on two distinct pathways (8, 14), several mutants isolated from budding and fission yeasts that are defective in DNA damage checkpoints also show sensitivity to hydroxyurea (an S-phase inhibitor), suggesting that the S-phase feedback control and the G_2/M-phase DNA damage checkpoint require many of the same gene products (3, 12, 25, 26, 40, 50).

Genetic evidence from studies of fission yeast has suggested that the replication complex is a possible source of the S-M-phase checkpoint (6, 7, 9, 11, 23, 27, 28, 35, 42). However, little is currently known about the biochemical mechanisms underlying the S-M-phase checkpoint and how checkpoint signals are transduced to the mitotic cyclin-dependent kinase p34^{cdc2}. To begin to elucidate these mechanisms, we sought to define a physiological condition of a fission yeast strain that delays S-phase progression. Mutagenesis of such a strain would allow us to identify gene products that are involved in generating and transducing checkpoint signals to prevent premature mitotic entry during the S-phase delay. To this end, we made use of a fission yeast strain that contains a thermosensitive allele of DNA polymerase δ (16) and defined a growth condition under which this enzyme is semidisabled, causing a delay of S-phase progression. By mutagenesis of this strain and subsequent screening for clones that die rapidly under the semipermissive conditions, we isolated a panel of mutants that fail to prevent premature mitosis when S phase is delayed. In this report, we describe the *aya14* mutant. Genetic analysis indicated that *aya14* is a novel mutant allele of a previously identified checkpoint *rad* gene, *rad26* (3). Results of our study suggest that this specific *rad26* allele causes cells to bypass S-phase arrest and enter mitosis prematurely. Moreover, *aya14* mutant cells preferentially bypass early S-phase arrest and advance into mitosis. A model of how the *rad26*$^+$ gene product functions in S-phase feedback control and how it coordinates with other checkpoint *rad* gene products in the G_2/M DNA damage checkpoint is proposed.

MATERIALS AND METHODS

Strains, media, and genetic and molecular techniques. *S. pombe* strains used in this study are listed in Table 1. The rich medium (YE) and Edinburgh minimal medium used (EMM) were as described in reference 18. Cells grown in YE medium were supplemented with 0.1 mg of adenine/ml (YEA) and/or with 1 μM thiamine (YEAT). Cells grown in EMM were supplemented with nutritional supplements (adenine, leucine, and uracil) and where appropriate with 1 μM thiamine (EMMT). These growth conditions were used for analyzing mutagenesis and for the mutant screen. For primary characterization of mutant clones and all other experiments, cells were grown either in EMM with appropriate nutritional supplements or in a rich medium (YES) with nutritional supplements (adenine, uracil, and leucine). For conjugation and sporulation, standard ME or MSA medium was used (31). All standard genetic procedures were performed as previously described (18, 31). Molecular biological techniques were as described in reference 30.

Analysis of growth rates. Growth rates were measured by diluting exponentially growing cells (0.5×10^7 to 1.5×10^7 cells/ml) to 2×10^6 cells/ml in appropriate medium and incubating them under various conditions. When ap-

* Corresponding author.

TABLE 1. Strains used in this study

Strain	Genotype	Reference or source
SP808	*h*$^+$ *ura4-D18 leu1-32 ade6-M216*	D. Beach
SP812	*h*$^-$ *ura4-D18 leu1-32 ade6-M210*	D. Beach
SF02	*h*$^+$ *polδts02 ura4-D18 leu1-32 ade6-M216*	16
SF03	*h*$^+$ *polδts03 ura4-D18 leu1-32 ade6-M216*	16
aya14	*h*$^+$ *rad26.a14 ura4-D18 leu1-32 ade6-M210*	This study
DB13	*h*$^+$ *polα::his3::polαts13 ura4-D18 leu1-32 ade6-M210*	5a
rad26.T12	*h*$^-$ *rad26.T12 ura4-D18 leu1-32 ade6-M704*	A. M. Carr and T. Enoch
aya14 polδts02	*h*$^+$ *rad26.a14 polδts02 ura4-D18 leu1-32 ade6-M216*	This study
aya14 polδts03	*h*$^+$ *rad26.a14 polδts03 ura4-D18 leu1-32 ade6-M216*	This study
aya14 polαts13	*h*$^+$ *ad26.a14 polα::his3::polαts13 ura4-D18 leu1-32 ade6-M210*	This study
aya14 cdc10	*h*$^+$ *rad26.a14 cdc10-129 ura4-D18 leu1-32 ade6-M210*	This study
aya14 cdc17	*h*$^-$ *rad26.a14 cdc17-K42 ura4-D18 leu1-32 ade6-M216*	This study
aya14 cdc20	*h*$^-$ *rad26.a14 cdc20-M10 ura4-D18 leu1-32 ade6-M210*	This study
aya14 cdc21	*h*$^-$ *rad26.a14 cdc21-M68 ura4-D18 leu1-32 ade6-M210*	This study
aya14 cdc22	*h*$^+$ *rad26.a14 dc22-M45 ura4-D18 leu1-32 ade6-M210*	This study
aya14 cdc24	*h*$^+$ *rad26.a14 cdc24-M38 ura4-D18 leu1-32 ade6-M210 can1-1*	This study
aya14 cdc25	*h*$^+$ *rad26.a14 cdc25-22 ura4-D18 leu1-32 ade6-M210*	This study
aya14 cdc27	*h*$^+$ *rad26.a14 cdc27-K3 ura4-D18 leu1-32 ade6-M216*	This study
aya14 wee1-50	*h*$^+$ *rad26.a14 wee1-50 ura4-D18 leu1-32 ade6-M210*	This study
aya14 chk1Δ	*h*$^+$ *rad26.a14 chk1Δ ura4-D18 leu1-32 ade6-M210*	This study
aya14/rad26Δ	*h*$^+$*/h*$^-$ *rad26.a14/rad26::ura4 ura4-D18/ura4-D18 leu1-32/leu1-32 ade6-M210/ade6-M216*	This study
aya14/rad26$^+$	*h*$^+$*/h*$^-$ *rad26.a14/rad26*$^+$ *ura4-D18/ura4-D18 leu1-32/leu1-32 ade6-M210/ade6-M216*	This study
rad26Δ polδts03	*h*$^-$ *polδts03 rad26::ura4 ura4-D18 leu1-32 ade6-M704*	This study
cdc2-3w polδts03	*h*$^+$ *polδts03 cdc2-3w ura4-D18 leu1-32 ade6-M210*	This study
rad3Δ wee1-50	*h*$^-$ *wee1-50 rad3::ura4 ura4-D18 leu1-32 ade6-M704*	This study
chk1Δ polδts03	*h*$^-$ *polδts03 chk1::ura4 ura4-D18 leu1-32 ade6-M704*	This study
chk1Δ polαts13	*h*$^+$ *chk1Δ polα::his3::polαts13 ura4-D18 leu1-32 ade6-M210*	This study
chk1Δ cdc10	*h*$^+$ *chk1Δ cdc10-129 ura4-D18 leu1-32 ade6-M210*	This study
chk1Δ cdc17	*h*$^-$ *chk1Δ cdc17-K42 ura4-D18 leu1-32 ade6-M216*	This study
chk1Δ cdc20	*h*$^-$ *chk1Δ cdc20-M10 ura4-D18 leu1-32 ade6-M210*	This study
chk1Δ cdc21	*h*$^-$ *chk1Δ cdc21-M68 ura4-D18 leu1-32 ade6-M210*	This study
chk1Δ cdc22	*h*$^+$ *chk1Δ cdc22-M45 ura4-D18 leu1-32 ade6-M210*	This study
chk1Δ cdc24	*h*$^+$ *chk1Δ cdc24-M38 ura4-D18 leu1-32 ade6-M210 can1-1*	This study
chk1Δ cdc27	*h*$^+$ *chk1Δ cdc27-K3 ura4-D18 leu1-32 ade6-M216*	This study

propriate, the cells were diluted in small increments to maintain growth in the exponential phase. Cell samples were collected at defined intervals and fixed in 30% ethanol for measuring cell number and for cytology analysis. Data shown in this study represent the averages of at least three independent experiments.

Cytological analysis. Cells were fixed in 30% ethanol and stained by direct addition of 4′,6-diamidino-2-phenylindole (DAPI) to a final concentration of 5 μg/ml for 20 min, followed by the addition of calcofluor to a concentration of 1.5 μg/ml for 3 min. The stained cells were then washed in phosphate-buffer saline (PBS), resuspended in an appropriate volume of PBS, and examined and photographed with a Nikon epifluorescence microscope.

Mutagenesis and mutant screen. Strain SF03 was mutagenized to 40% viability with 0.15% ethyl methanesulfonate. One-half million cells (5×10^5 cells) were plated on YEAT and incubated at 25°C for 5 days (master plate). The surviving colonies were then replica plated onto EMMT supplemented with 3 μg of phloxine B/ml. After incubation at 33°C overnight (tester plate), colonies which stained red (dead) were identified, fixed in 30% ethanol, and stained with DAPI and calcofluor to examine the nuclear morphology. Clones that had greater than 30% of cells displaying abnormal nuclear phenotypes were selected as candidates for the S-M-phase checkpoint mutants. The candidate clones were then isolated from the master plates and subjected to three additional rounds of screening. Clones that reproducibly fulfilled the criteria of lethality at 33°C on EMMT plates and displayed >30% abnormal nuclear morphology were selected.

Hydroxyurea sensitivity analysis. Cells were plated onto solid medium (YES) containing 6 mM hydroxyurea and 3 μg of phloxine B/ml. Sensitivity was estimated by the extent of mortality (red color and/or poor growth) compared to wild type. Hydroxyurea sensitivity assays in liquid medium were performed by first inoculating log-phase-growing cells in YES medium at a density of 2×10^6 to 3×10^6/ml (0.2 optical density units at 595 nm) and allowing the cells to grow for 1 h at 30°C. Hydroxyurea was then added to a concentration of 10 mM. A fixed number of cells were removed at defined intervals, diluted, and plated onto YES plates and incubated at 30°C for 2 to 3 days. Colonies were scored, and survival was expressed as a percentage of the colonies which formed on samples plated immediately before the addition of hydroxyurea. From the same cultures, specimens were also fixed and stained for cytology analysis.

UV survival analysis. A known density of logarithmically growing cells was plated onto appropriate agar plates and exposed to doses of UV light from 0 to 300 J/m^2. Plates were incubated at 30°C for 4 to 5 days. UV sensitivity was measured as a percentage of the colonies which formed on equivalent plates that were not irradiated with UV light.

γ irradiation analysis. The extent of gamma irradiation sensitivity was measured by exposing a liquid culture at a density of 5×10^3 cells ml^{-1} in YE medium to a ^{137}Cs source (11 Gy min^{-1}). At set doses, cell samples were removed and plated. After being incubated for 3 to 4 days at 30°C, colonies were counted and survival was expressed as a percentage of the colonies which formed on plates that were not exposed to irradiation.

Isolation of the *aya14* gene and suppressor. The *aya14* mutant strain was transformed with the pURSP2 genomic library (5). Transformed cells (>100,000 independent colonies) were plated on selective EMM medium containing 10 mM hydroxyurea. Hydroxyurea-resistant colonies were picked and verified by three rounds of selection on hydroxyurea medium. Plasmids from the hydroxyurea-resistant colonies were recovered and further verified by transformation into the *aya14 cdc22* double mutant to test their ability to rescue the growth of the *aya14 cdc22* strain at the semipermissive temperature of the *cdc22* strain (34°C). Two plasmids that rendered the *aya14* mutant hydroxyurea resistant and also supported growth of the *aya14 cdc22* strain at 34°C were obtained. These two plasmids were sequenced and compared to known sequences in the gene bank.

Identification of *rad26.a14* mutation. Genomic DNA was prepared from the *aya14* strain as previously described (22) for use as a PCR template. Three sets of primers were used to isolate three 1-kb fragments of *rad26*$^+$ by PCR. Primers for the isolation of the N-terminal portion of *rad26*$^+$ were 5′-ATCGATCCCG CATAAACGAGAGTGAAAGC-3′ and 5′-CGGAGGAAACGATATTGTAG GACGTCAGTG-3′. Primers for the isolation of the central portion of the *rad26*$^+$ gene were 5′-ATCGGATCCATCCCATGAAGATGGTGAC-3′ and 5′-CTTACTTACCTATTGCAAGTGACGTCAGTG-3′. Primers for the isolation of the C-terminal portion of the *rad26*$^+$ gene were 5′-ATCGGATCCGCCTCC TTTGCTATAACATC-3′ and 5′-CTTTGTCTACTTAGATAAAGGGCGTCA GTG-3′. All three PCR products were cloned into pUC18 at the *Bam*HI and *Pst*I sites and sequenced.

Flow cytometry analysis. Cells were harvested, washed in water, and fixed in 70% ethanol prior to staining with either chromomycin 3A as previously described (43) or propidium iodide as previously described (37). DNA content was determined by a Coulter fluorescence-activated cell sorter.

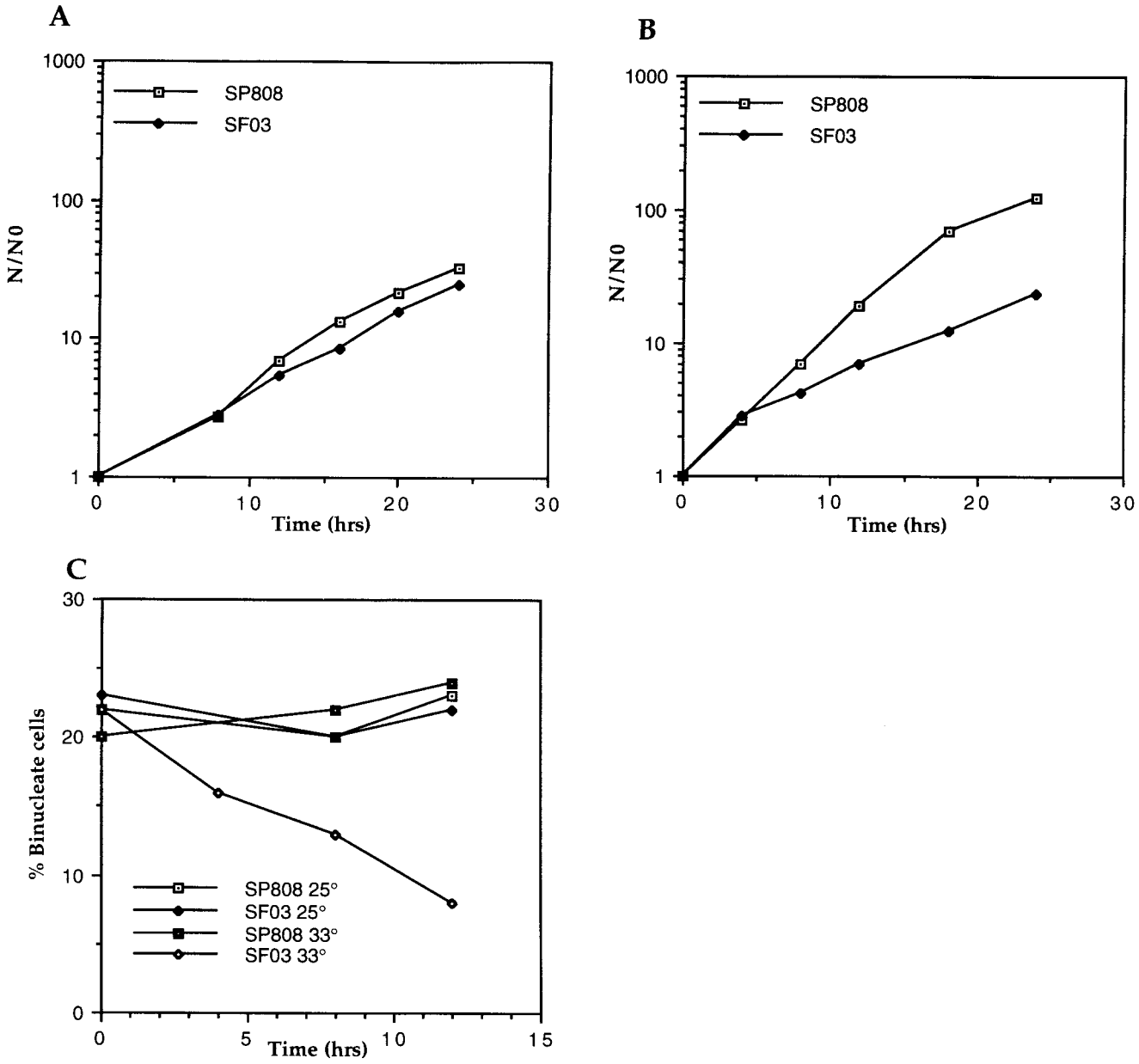

FIG. 1. A semipermissive condition for SF03 under which DNA polymerase δ is semidisabled. Growth rates and DNA contents of wild-type SP808 and mutant SF03 cells were measured as described in Materials and Methods. Data represent the averages of three independent experiments. Cell counts were normalized to the input cell number (N_0). (A) Permissive conditions. (B) Semipermissive conditions. Cells were grown at 25°C to mid-log phase and then shifted to 33°C at time zero. (C) Percentage of cells in mitosis. Data are percentages of single cells containing two nuclei as determined with a microscope.

RESULTS

Conditions under which DNA polymerase δ is semidisabled cause an S-phase delay. *S. pombe* mutant strain SF03, which carries a temperature-sensitive allele, *polδts03*, of DNA polymerase δ, was used to identify the S-M-phase checkpoint genes that detect a delay in S-phase progression. At the restrictive temperature, SF03 arrests in S phase with a *cdc* phenotype (16). A semipermissive condition for the SF03 strain was empirically defined by assessing the effects of different temperatures and nutrient compositions on its growth kinetics. The goal was to find a condition under which DNA polymerase δ in SF03 is partly disabled, thus causing a delay, but not an arrest, in S-phase progression.

At 25°C in EMMT, as well as in YEAT, SF03 and the parental wild-type strain SP808 have identical growth rates, with an average doubling time of 3.5 h (Fig. 1A). However, in EMMT at 33°C, while the wild-type strain SP808 has a doubling time of 3 h and shows a typical 2C DNA content, SF03 has a growth rate slower than that of the wild type, with a doubling time of 4 h (Fig. 1B). To test whether the increase in doubling time of SF03 under these conditions is not due to the proportion of dead cells, the viability of SF03 cells grown at the semipermissive conditions was analyzed by plating a known number of cells at the permissive conditions. Results indicated that cells were viable for 24 h under the semipermissive conditions. Furthermore, when SF03 cells were directly plated on

TABLE 2. Phenotypes of known checkpoint mutants in a *polδts03* background

Strains	Permissive conditions[a]	Semipermissive conditions[b]
cdc2-3w polδts03	++	*cut* phenotype
rad3Δ polδts03	Synthetic lethal	NA
rad26Δ polδts03	+	*cut* phenotype
chk1Δ polδts03	++	*cut* phenotype

[a] ++, no growth defect; +, mild growth defect.
[b] *cut* phenotype represents various abnormal nuclear morphologies. NA, not applicable.

phloxine B agar and grown at the semipermissive conditions, cells formed white colonies with a moderate increase in cell length (data not shown). These results suggest that the increase in doubling time of SF03 under the semipermissive conditions is not due to cell death. To further clarify the slower growth rate observed in EMMT at 33°C, we assessed the percentage of SF03 cells completing mitosis by quantitating the binucleated single cells (Fig. 1C). Exponentially growing SP808 or SF03 cells completed mitosis at a steady state rate of 20% in rich medium at 25°C. In EMMT at 33°C, SF03 cells showed a gradual decrease of binucleated cells from 20% to less than 10% (Fig. 1C).

Results of these analyses strongly suggest that in EMMT at 33°C, the cell cycle of SF03 is delayed. The cause of the cell cycle delay is the *polδts03* allele of the principal DNA elongation enzyme, DNA polymerase δ (47). The growth conditions of SF03 are thus defined as follows: (i) the permissive conditions are YEAT (or EMMT) at 25°C, and (ii) the semipermissive conditions, which cause a delay of S phase, are EMMT at 33°C.

Genetic screen for mutants that undergo premature mitosis when S phase is delayed. The strategy of our genetic screen is to use synthetic lethality to identify mutants that fail to detect the incomplete DNA replication caused by the semidisabled polymerase δ. To test the validity of this genetic strategy, four known checkpoint mutants, *rad3Δ*, *rad26Δ*, *chk1Δ*, and *cdc2-3w*, were crossed into a *polδts03* genetic background to determine their viability and phenotypes under the semipermissive conditions of SF03. The *rad3Δ polδts03* double mutant was synthetic lethal under the permissive conditions. This may be due to a slight growth defect of SF03 at the permissive conditions. Consequently, the function of $rad3^+$ becomes essential for normal cell growth at the permissive conditions. The *cdc2-3w polδts03* and *chk1Δ polδts03* double mutants had normal growth at permissive conditions, whereas at the semipermissive conditions, these two double mutants both displayed an abnormal "*cut*" nuclear phenotype. The *rad26Δ polδts03* double mutant grew poorly at the permissive conditions and died rapidly with a *cut* nuclear morphology at the semipermissive conditions (Table 2). These results indicate that the genetic screen with the *polδts03* allele at the semipermissive conditions is able to identify checkpoint mutants.

S. pombe SF03 was mutagenized with ethyl methanesulfonate to 40% viability. The criteria for the isolation of S phase to mitosis checkpoint mutants are (i) clones are viable under the permissive conditions, and (ii) under the semipermissive conditions, clones are synthetic lethal with the *polδts03* allele and have at least 30% of cells displaying aberrant mitotic nuclear morphologies. A total of 29 mutant clones that fulfilled these criteria were isolated and verified. Complementation analyses have shown that these mutants fall into seven complementation groups (Table 3). Since the parental strain SF03 is slightly sensitive to hydroxyurea, mutants were crossed into the $polδ^+$ background in order to test their hydroxyurea sensitivity. Most of these mutants were found to be sensitive to 5 mM hydroxyurea but none were sensitive to UV irradiation of up to 100 J/m^2 (Table 3). This suggests that the criteria used for the screen had primarily identified genes that detect incomplete DNA replication rather than DNA damage. Two complementation groups of the mutants, class I and class VI, are highly sensitive to hydroxyurea. Class I and class III mutants constantly have a background of 10 to 20% of cells with the *cut* nuclear morphology at the permissive conditions (Table 3). These two groups of mutants are similar to the *hus5* mutant which also displays a constant *cut* phenotype (2, 12). Genetic crosses, however, indicated that neither class I nor class III mutants were *hus5* mutants. Diploids heterozygous for each of the mutants were constructed with SF03 and tested for their lethality at the semipermissive conditions. All of these mutants were found to be recessive of their phenotypes.

TABLE 3. Complementation analysis of mutants

Class	Representative mutant	Nuclear morphology	Hydroxyurea sensitivity[a]	UV irradiation sensitivity[b]
I	*aya1*	Constant *cut*	++	−
II	*aya5*	Polarity defect	ND	−
III	*aya6*	Constant *cut*	+	−
IV	*aya7*	*cut* and anucleate	−	−
V	*aya13*	Anucleate	ND	−
VI	*aya14*	Anucleate	++	−
VII	*aya26*	Missegregate	−	−

[a] Hydroxyurea sensitivity analysis was performed on mutants in wild-type $polδ^+$ background at 30°C in YES medium containing 5 mM hydroxyurea. ++, sensitive; +, moderately sensitive; −, not sensitive; ND, not determined.
[b] UV irradiation sensitivity analysis was performed on mutants in a *polδts03* background with a UV dose of 100 J/m^2 at 25°C.

The abnormal nuclear phenotypes of these mutants under the semipermissive conditions for *polδts03* can be grouped into four types (Fig. 2), although some mutants display pleiomorphic phenotypes. The first type displays the classic *cut* phenotypes, resulting from cells attempting to undergo mitosis and cytokinesis with incompletely replicated and segregated chromosomes (Fig. 2A) (21). The second type displays anucleate cells, in which the genetic material is segregated unevenly between the daughter cells (Fig. 2B). The third type shows an

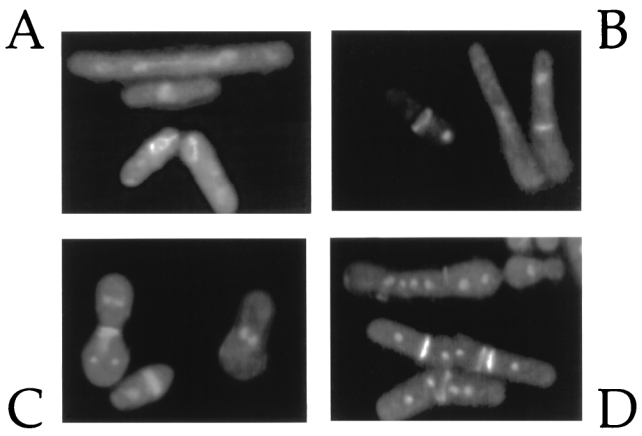

FIG. 2. Phenotypes of mutant clones. The S-phase feedback control mutant clones isolated by the genetic screen described in this study displayed one or more of the following phenotypes: *cut* (A), anucleate (B), abnormal polarity (C), and random or missegregate nuclear materials (D).

abnormal nuclear material segregation termed the "polarity phenotype," in which mitotic segregation occurs across rather than along the axis of the cell (Fig. 2C). Since these cells did not arrest with an elongated cell morphology, they were selected as potential checkpoint mutants. The fourth type appears to have a random segregation of highly condensed *S. pombe* nuclear materials between the daughter cells, which is termed the "missegregate" phenotype (Fig. 2D). The first two types of nuclear morphology are examples of the classic mitiotic catastrophe nuclear phenotype. It is not clear whether the DAPI staining materials shown in the polarity and missegregated phenotypes represent the nucleus or the chromosome. We named these mutant phenotypes *aya* for abnormalities in yeast cell cycle arrest. In this study, we describe the characterization of the *aya14* mutant.

Primary characterization of the *aya14* mutant. Under the semipermissive conditions, the *aya14* mutant in a *pol*δ*ts03* background had 30% of cells displaying the anucleate phenotype. To test whether the observed *aya14* phenotype is due to a single mutation, we successively backcrossed the *aya14 pol*δ*ts03* strain to the wild-type SP812 three times. The resulting strain was hydroxyurea sensitive but not temperature sensitive. The *aya14* mutant in the wild-type *pol*δ$^+$ background was also successively crossed three times with SF03 containing the *pol*δ*ts03* allele to confirm the synthetic lethality at the semipermissive conditions. The synthetic lethality of the *aya14* mutant in the *pol*δ*ts03* background remained; thus the *aya14* phenotype is due to a single mutation. All of the experiments described hereafter were performed with the *aya14* mutant in the wild-type *pol*δ$^+$ background unless otherwise designated.

We first tested the viability of the *aya14* strain in 10 mM hydroxyurea in comparison to that of the wild-type strain SP812, the parental SF03 (harboring the *pol*δ*ts03* allele), and the S-M-phase-checkpoint-defective *rad3*Δ strain (Fig. 3A). Wild-type cells were fully viable after 6 h in hydroxyurea. Strain SF03 containing the mutant allele *pol*δ*ts03* was slightly sensitive to hydroxyurea, with more than 50% of cells viable after 6 h in hydroxyurea. As previously characterized, the *rad3*Δ mutant was highly sensitive to hydroxyurea, with no viable cells after 4 h in hydroxyurea (1). The strain containing the *aya14* mutation was also sensitive to hydroxyurea, with 5% of viable cells after 6 h in 10 mM hydroxyurea. The sensitivity of the *aya14* mutant to hydroxyurea was found to be directly proportional to the abnormal nuclear morphology observed after growth in hydroxyurea. Both wild-type SP812 and SF03 had negligible percentages of cells with abnormal nuclear morphologies after 6 h in 10 mM hydroxyurea, whereas more than 80% of the *rad3*Δ mutant cells and 70% of the *aya14* mutant cells showed abnormal mitotic nuclear morphologies (Fig. 3A). The *aya14* mutant predominantly displayed anucleate nuclear morphology (Fig. 3B), while the *rad3*Δ mutant displayed both *cut* and anucleate nuclear morphologies. To further verify that the *aya14* strain was able to enter premature mitosis when S phase was inhibited, the strain was crossed into a *cdc22* background which encodes the large subunit of ribonucleotide reductase (RNR) (15). At the restrictive temperature, the percentage of cells displaying an abnormal nuclear morphology was examined. Similar to that observed when S phase was blocked by hydroxyurea, after 6 h at 36°C, at least 40% of *aya14* cells displayed the anucleate phenotype (see description below in Table 4).

We then compared the UV sensitivities of the *aya14* strain, the wild-type SP812, the parental SF03, and the *rad3*Δ mutant (Fig. 3C). The *aya14* strain was similar to wild-type SP812 and SF03 in having more than 70% viable cells after irradiation of up to 100 J/m^2, whereas the *rad3*Δ strain had less than 0.1% viable cells. After irradiation at a dose of 100 J/m^2 the *aya14* and wild-type cells showed a moderately elongated cell morphology but no abnormal nuclear morphology, suggesting that the DNA damage checkpoints in these two strains were intact. In contrast, *rad3*Δ cells did not show any elongated cell morphology but had a high percentage of cells displaying the *cut* nuclear morphology (data not shown). At 150 J/m^2, the *rad3*Δ strain had no viable cells and the *aya14* strain had an identical sensitivity to that of the wild-type cells (40% viability), while SF03, surprisingly, showed a higher sensitivity to UV irradiation (10% viable cells). SF03 consistently had a higher sensitivity to UV than the wild type and the *aya14* strain at 200 and 300 J/m^2. These results indicate that the UV sensitivity of cells with the *aya14* mutation is similar to that of the wild-type SP812 and is less sensitive to UV than its parental strain, SF03, but it is strikingly different from cells with the *rad3*Δ mutation.

The *aya14* strain was further analyzed for its sensitivity to γ irradiation and compared to the *rad3*Δ, SP812, and SF03 strains (Fig. 3D). At 100 Gy, the *rad3*Δ strain had no viable cells. In contrast, the *aya14* strain, similar to wild-type SP812 and SF03, was fully viable. Similar to that observed in the UV radiation analysis, SF03 showed a slightly higher sensitivity to γ irradiation than did the *aya14* strain. At 750 Gy, 60% of wild-type cells remained viable, while the *aya14* strain had approximately 30% viable cells and SF03 had about 10% viable cells, suggesting that the *aya14* strain is not significantly sensitive to γ irradiation.

To test if G_2 arrest rescues the viability of the *aya14* strain in hydroxyurea, we crossed the *aya14* mutant into a *cdc25* background. The *aya14 cdc25* double mutant was first grown in 10 mM hydroxyurea at the permissive temperature for 2 h to block the progression of S phase. After 2 h in hydroxyurea, the cell cycle arrest of the *aya14 cdc25* strain was confirmed by flow cytometry analysis, showing a majority of cells with a 1C DNA content (data not shown). The double mutant was then shifted to 36°C, the restrictive temperature for the *cdc25* strain. While the *aya14* single mutant progressively lost viability at 36°C after 6 h due to inappropriate mitotic entry, the *aya14 cdc25* double mutant remained viable throughout 6 h in 10 mM hydroxyurea at 36°C (Fig. 3E). This result shows that G_2 arrest due to the *cdc25* mutation prevents the *aya14* strain from entering premature mitosis when S phase is inhibited by hydroxyurea.

Fission yeast *rad*Δ and *hus* mutants are synthetic lethal in the *wee1* mutant background (1–3). To test the viability of the *aya14* strain in a *wee1* genetic background, a diploid *aya14/wee1-50* strain was constructed. A *rad3*Δ *wee1-50* double mutant was constructed as a control. Upon sporulation followed by tetrad dissection, nine haploids containing *aya14 wee1-50* double mutations were analyzed. To ensure that the mutant cells contained mutations in both *aya14* and *wee1-50,* all nine haploids were backcrossed with wild-type SP812. Resulting haploids displayed classic tetrad-type in hydroxyurea sensitivity assays and the temperature-sensitive Wee$^-$ phenotype (34), indicating that the cells were *aya14 wee1-50* double mutants. Following a temperature shift to 36°C, *aya14 wee1-50* double mutant cells were fully viable for up to 8 h (Fig. 3F). In contrast, *rad3*Δ *wee1-50* double mutant cells were only 20% viable under the same condition. These results indicate that *aya14* is not synthetic lethal in the *wee1* mutant background. Thus, the *aya14* mutant is different from many potential checkpoint and/or feedback control mutants previously described (1–3, 12, 26, 40).

***aya14* is a novel mutant allele of *rad26*.** Finding that the *aya14* mutant is not synthetic lethal in a *wee1-50* background suggests that the *aya14* mutant is not one of the previously identified *rad* and *hus* mutants (3). To ensure the distinct

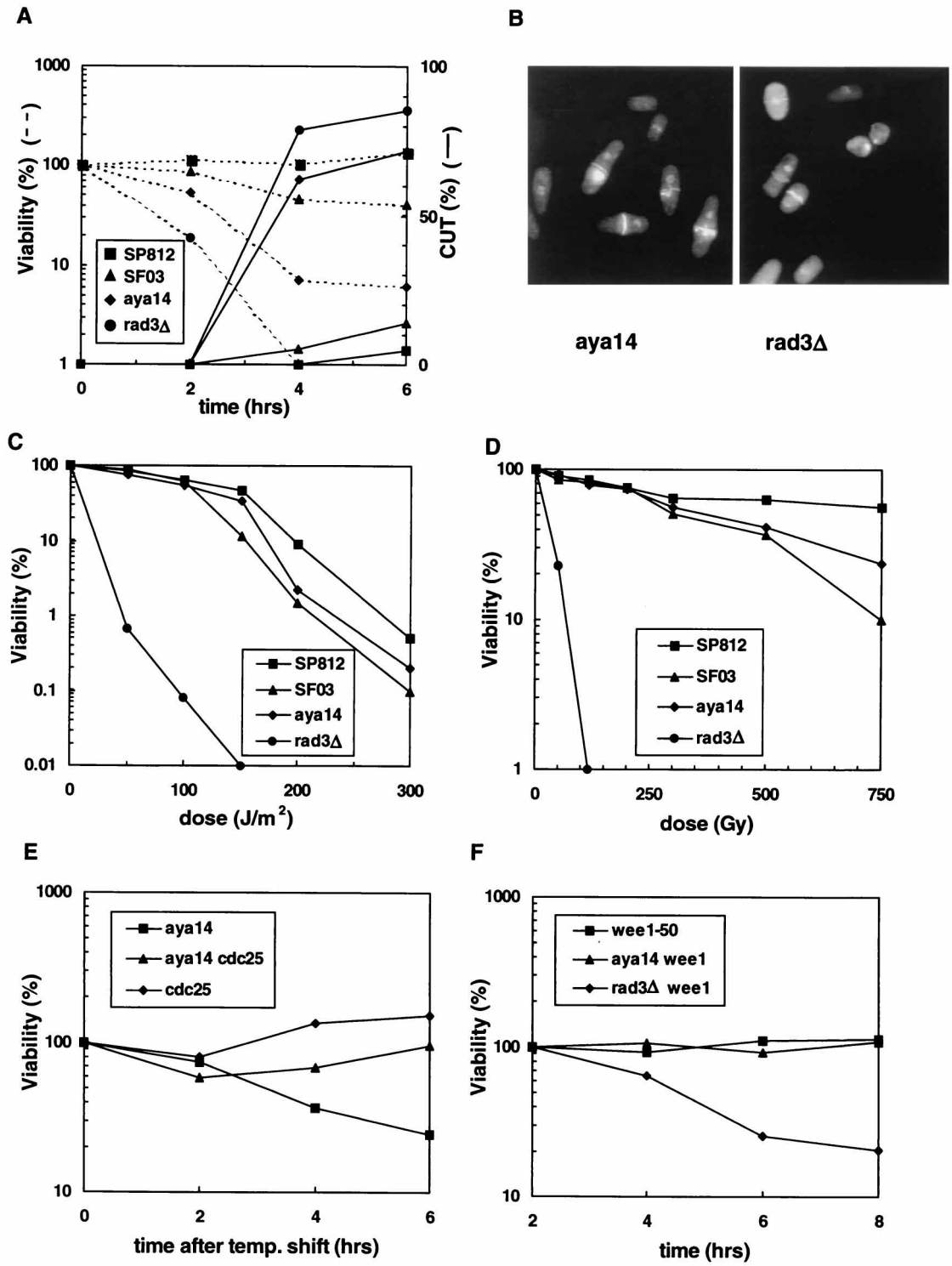

FIG. 3. Characterizations of the *aya14* mutant. Viability, radiation survival, and epistasis analysis were determined as described in the Materials and Methods. (A) Viability of the *aya14* mutant and percentage of cells entering premature mitosis described as *cut* in 10 mM hydroxyurea. (B) DAPI and calcofluor staining of *aya14* and *rad3*Δ mutants after 6 h in 10 mM hydroxyurea at 30°C. (C) UV radiation survival of *aya14* mutant compared to wild-type SP812, parental strain SF03, and *rad3*Δ mutant (D) γ radiation survival of *aya14* mutant compared to wild-type SP812, SF03, and *rad3*Δ mutant (E). Rescue of the *aya14* S-phase feedback control defect by G_2 arrest. Viability of the double mutant was measured after a shift to 36°C and compared to that of the *aya14* and *cdc25* single mutant strains. (F) *aya14* mutant is viable in *wee1* genetic background. *aya14 wee1-50* double mutant was first grown at 25°C to mid-log phase and then shifted to 36°C. Since *wee1-50* continued to grow for 2 h after the shift to 36°C, the viabilities of the *aya14 wee1-50* and *rad3*Δ *wee1-50* double mutants were normalized to the viability of *wee1-50* at 2 h after the shift to the restrictive temperature.

identity of the *aya14* mutant, we constructed diploid strains containing *aya14* and *hus1*, *hus2*, *hus3*, *hus4*, *hus5*, *hus6*, *rad1*Δ, *rad3*Δ, *rad9*Δ, *rad17*Δ, *rad24*Δ, *rad25*Δ, *rad26*Δ, *chk1*Δ, *cdc10*, *cdc22*, *cdc25*, or *cdc2-3w*, and the resulting progenies derived from each diploid were analyzed for their sensitivity to hydroxyurea. With the exception of *rad26*Δ, all *aya14/rad* or *aya14/hus* diploids had more than 20% hydroxyurea-resistant wild-type spores, indicating that the *aya14* mutant is not one of these *rad* or *hus* mutants. Surprisingly, sporulation of *aya14/rad26*Δ yielded less than 0.1 to 0.2% haploids that survived in hydroxyurea. Since the *rad26* gene disrupted by *ura4*$^+$ has most of the C-terminal portion of the gene intact (3), the 0.1 to 0.2% of hydroxyurea-resistant haploids might result from an intragenic recombination. We further constructed a diploid strain containing *aya14* and *rad26.T12* (3). The *aya14/rad26.T12* diploid yielded no wild-type-like hydroxyurea-resistant daughter cells. This result suggests allelism between *aya14*$^+$ and *rad26*$^+$. To further verify this, we constructed two diploids, *aya14/rad26*Δ and *aya14/rad26*$^+$, and tested their hydroxyurea sensitivity. On a plate with 6 mM hydroxyurea, the *aya14/rad26*$^+$ diploid grew normally, whereas the *aya14/rad26*Δ diploid was unable to grow (Fig. 4A). It has been reported that the *rad26*Δ mutant is considerably more sensitive to DNA damage agents than the *rad26.T12* mutant and that *rad26.T12* cells in a *chk1*Δ (*rad27*Δ) background are highly sensitive to UV irradiation (3). We therefore tested the UV sensitivity of the *aya14 chk1*Δ double mutant in order to test the relationship between the *rad26.T12* and *aya14* strains. As shown in Fig. 3C, both the *aya14* single mutant and the wild-type SP812 were not sensitive to UV irradiation of up to 200 J/m^2. The *rad26*Δ mutant showed a high sensitivity to UV irradiation (3). The strain with *chk1*Δ showed a moderate sensitivity to UV irradiation with a higher sensitivity than the wild type and the *aya14* strain, similar to that which was reported previously (2). The *aya14 chk1*Δ double mutant showed a similar sensitivity to UV irradiation to that of the *rad26*Δ mutant (Fig. 4B) and the *rad26.T12 chk1*Δ double mutant (data not shown). We further compared the γ radiation sensitivity of the *aya14* and *rad26.T12* strains. The *aya14* strain was found to be significantly less sensitive to γ radiation than was the *rad26.T12* strain (data not shown). These results strongly suggest that *aya14* and *rad26* are allelic; however, *aya14* is a different mutant allele from *rad26.T12.*

To verify the allelism of *aya14* and *rad26*, the *aya14* mutant strain was transformed with the pURSP2 genomic library (5), and the transformants were tested for hydroxyurea sensitivity. Two genomic clones of 3 and 3.5 kb were found to suppress the hydroxyurea sensitivity of the *aya14* strain. Sequence analysis indicated that one contains the *rad26*$^+$ gene (3) and the other contains the *cds1*$^+$ gene (32). To identify the *aya14* allele, genomic DNA of the *aya14* strain was isolated and used as a PCR template to isolate three 1-kb PCR fragments as described in Materials and Methods. To avoid possible PCR amplification artifacts, five clones from five independent PCR reactions were sequenced. Results indicated that in all five clones, *aya14* contains a tandem repeat of an insertion of 5′-AATCCCTTAATAGTATGC-3′ of *rad26*$^+$ (3). This insertion resulted in a repeat of a block of six amino acids, NPLIVC, in the C-terminal region of the *rad26*$^+$ gene product, Rad26 (Fig. 4C). This mutant allele is hereafter named *rad26.a14.*

***cds1*$^+$ suppresses the *rad26.a14* strain when S phase is inhibited by hydroxyurea or arrested by** *cdc22. cds1*$^+$ was originally identified as a multicopy suppressor of the temperature-sensitive allele *swi7-H4* of a DNA polymerase α mutant. This gene encodes a protein kinase motif and has been proposed to be a component of the S-M-phase checkpoint via interacting with DNA polymerase α (32). Finding that *cds1*$^+$ was able to rescue the hydroxyurea sensitivity of the *rad26.a14* strain (Fig. 5A) led us to further investigate the effect of *cds1*$^+$ on *rad26.a14* cells when S phase was arrested by a variety of *cdc* mutants that affect S-phase progression. *rad26.a14* was constructed into a *cdc22* background for a poststart arrest in G_1/S at 36°C (20, 36). The *rad26.a14 cdc22* double mutant transformed with vector alone did not recover from the G_1/S-phase arrest. The double mutant transformed with a *rad26*$^+$ genomic clone fully recovered from the *cdc22* temperature arrest, while a double mutant transformed with a *cds1*$^+$ genomic clone also recovered from the temperature arrest (Fig. 5B) with no apparent morphological difference between cells carrying *rad26*$^+$ or *cds1*$^+$. To test if *cds1*$^+$ is able to rescue the feedback control defect of the *rad26.a14* strain when S phase is arrested by cellular DNA polymerase mutants, *rad26.a14* was constructed into the *cdc20* genetic background (with a *polεts* background). At 36°C, *cdc20* arrests cells at G_1/S (20, 36); however, the *cdc20* strain does not lose viability at the restrictive temperature and can be fully recovered from the temperature arrest (44a). The *rad26.a14 cdc20* double mutant, independently transformed with vector alone or with a *rad26*$^+$ or a *cds1*$^+$ genomic clone, was incubated at 36°C continuously for 48 h to arrest at G_1/S phase. Again, the *rad26.a14 cdc20* double mutant transformed with *rad26*$^+$ was viable at the restrictive temperature (Fig. 5C). In contrast, the double mutant transformed with *cds1*$^+$, similar to that transformed with vector alone, was inviable (Fig. 5C) and showed an abnormal mitotic nuclear phenotype (Fig. 5D). Similar results were obtained with *rad26.a14 polδts02* (with *polδts* background) (16) and *rad26.a14 polαts13* (with *polαts* background) (5a) double mutants transformed with *cds1*$^+$ at 36°C. Thus, *cds1*$^+$ is a multicopy suppressor for the hydroxyurea sensitivity of the *rad26.a14* strain and the defect of the *rad26.a14* strain only when S phase is inhibited by *cdc22*. Interestingly, *cds1*$^+$ is unable to prevent the *rad26.a14* strain from bypassing the S-phase arrest induced by a replicative DNA polymerase mutant. In addition, *cds1*Δ is synthetic lethal with *cdc22-M45* at 25°C, and *cds1*Δ cells in different *cdc* mutant backgrounds when arrested at different stages of S phase did not display the mitotic catastrophe phenotype to any significant extent (44a).

The *rad26.a14* strain bypasses S-phase arrest but not prestart G_1 arrest or late S/G_2 arrest. The properties of the *rad26.a14* strain described above strongly suggest that mutation at this specific *rad26* allele causes a defect in preventing premature mitosis when S phase is delayed or arrested. To examine this further, several cell cycle mutants were used to arrest cells at G_1 prior to start, in late G_1 after start, and throughout S phase. *rad26.a14* double mutants in different *cdc* mutant backgrounds were constructed. Cells were arrested in prestart G_1 by *cdc10* (20); in poststart late G_1 and early S phase by *cdc22*, *cdc20*, *cdc21*, and *polαts13*; in S phase by *cdc24*; in late S phase by *polδts03*; and in late S/G_2 phase by *cdc27* (16, 36) and *cdc17*, which has been used to identify G_2/M damage checkpoint mutants (3). Since *chk1*$^+$ is an S-phase checkpoint effector (6, 46), we also introduced *chk1*Δ into these *cdc* mutant backgrounds to analyze their possible relations to *rad26.a14* at different stages of the cell cycle arrest. Results of all the *rad26.a14 cdc* double mutants are summarized in Table 4, and three representative *rad26.a14 cdc* double mutants are shown in Fig. 6.

By these analyses, less than 10% of *rad26.a14* cells in the *cdc10* background bypassed the prestart G_1 arrest, and >70% of cells were viable after 6 h at the restrictive temperature (Table 4 and Fig. 6A). These results suggest that *rad26.a14* is not required for the checkpoint at prestart G_1 to M phase. The 10% of cells that bypassed the prestart G_1 arrest could be due

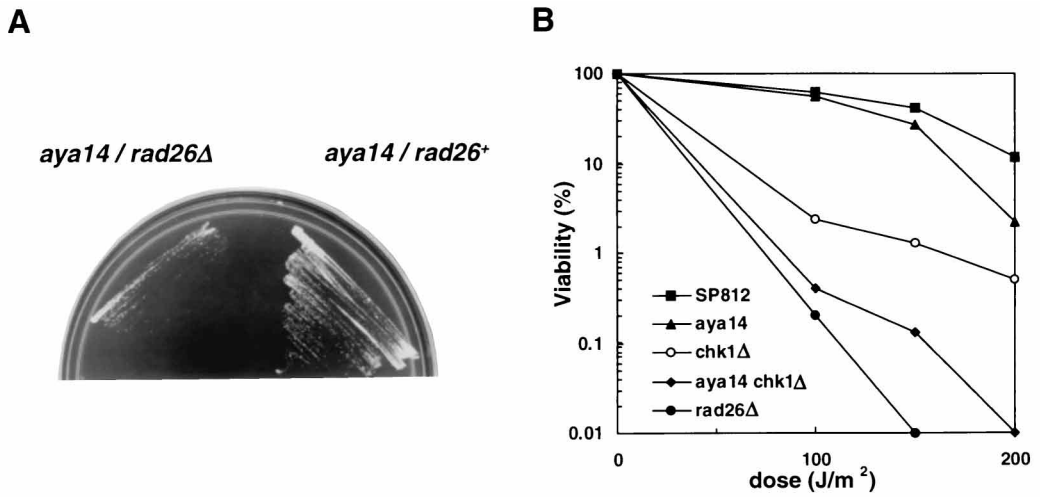

C

MMADESFDLE SLGSDEIFEG VNLDELEQQA QTQVQAQSSQ VVVPSEKQKQ
NLNLPNSYTN SSQKVRESTV NSQASLSSND LRTELLIKSG ENAILRANLL
KQSEANNAAL ESLNNSIKQK QDEYQRKLEE LKKEIEYAKT KSLFHEREAQ
DAIETMKKMK RDVKNSPIMK KSHEEDGDNK LLSSSDQLAK STKHAAKNSP
SKKKRKTSVA TAEDASTDSV SSSIAISDAS LSLSLMKDLL SLQKREDLYF
SSRTLAYVFG GCMHSLETIE GEEEGECLFN NLKALIYSPD LSMDSSNYVQ
SVVQTSSSIL NYSMKKLLYN ASFAITSLFN ALLILDPKSS TFIFQENVVS
LISGFLLKEY EKSNFLDSKF YVLIDFLYLY LSIARESADD FANITKAVDP
SLFESCIRVQ NAPSLIKCGV CLIISSTTPS FCASVNLLNA DDKSQESLMQ
LFTTMAHILV VTTRERINFP ELNEWITLHR FVISFFTVFI QMSGNIGKEI
LKVCNPLIVC **NPLIVC**IGLA ITWYHQQLLS SMYPQNECVE ILVSLVRLLY
ILSSEDLSSK FMLAENALQP RFVYAIACCA FGDTEQKAFG NLGEEMYFLT
TELLEVCVSP EELEQLYTNF

FIG. 4. *aya14* is a new mutant allele of *rad26*$^+$. (A) Hydroxyurea sensitivity of diploid *aya14/rad26*Δ and *aya14/rad26*$^+$ strains. Diploids were grown on EMM agar minus adenine but containing 6 mM hydroxyurea at 30°C for 5 days. (B) The *aya14* mutant in a *chk1*Δ genetic background is sensitive to UV irradiation. The UV sensitivities of the *aya14 chk1*Δ double mutant and the *aya14*, *chk1*Δ, and *rad26*Δ single mutants were compared to that of the wild-type SP812. (C) Sequence of *rad26* that contains the *rad26.a14* mutant allele. The predicted primary sequence of the *rad26* mutant is shown. The inserted six-amino-acid tandem repeat is shown in bold.

to a leak-through of *cdc10-129* to S phase. After a shift to the nonpermissive temperature, the *rad26.a14 cdc21* double mutant had approximately 50% of cells showing a DNA content of <2C but >1C and the other half of the cell populations with a DNA content of <1C (Fig. 6B). The *rad26.a14 cdc21* double mutant showed a progressive decrease of relative viability, and after 6 h nearly 80% of cells displayed an abnormal mitotic nuclear morphology (Fig. 6B and Table 4). Double mutants containing *rad26.a14* and *cdc20*, *cdc21*, or *pol*α*ts13* all showed a flow cytometry profile of early S phase after shift to the nonpermissive temperature and had from 70 to more than 80% of cells displaying abnormal mitotic nuclear morphology (Table 4). These findings indicate that the *rad26.a14* mutant had bypassed the early S-phase arrest imposed by these *cdc* mutants and undergone inappropriate mitosis. *rad26.a14 cdc* double mutants arrested with a late S-phase flow cytometry profile all had much lower percentages of cells displaying abnormal mitotic nuclear morphology (Table 4). The *rad26.a14 cdc27* and *rad26.a14 cdc17* double mutants arrested at the restrictive temperature at late S/G_2 with a 2C DNA content had only 15% of cells displaying abnormal mitotic nuclear morphology (Table 4); however, the cells were elongated, indicating that the

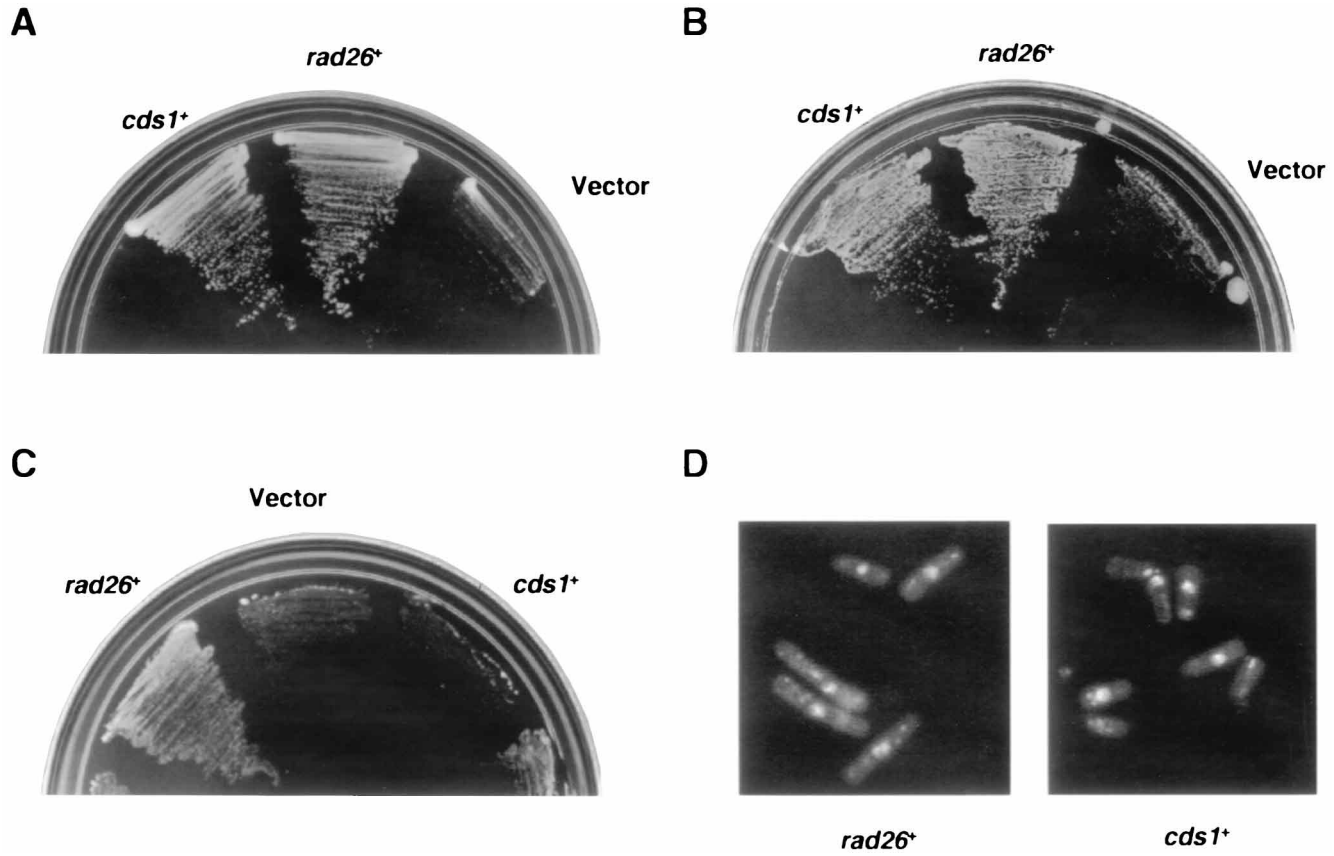

FIG. 5. *cds1*$^+$ suppresses *rad26.a14*. (A) *cds1*$^+$ suppresses the hydroxyurea sensitivity of the *rad26.a14 mutant. rad26.a14* cells independently transformed with pUR19 vector, pUR19-*rad26*$^+$, or pUR19-*cds1*$^+$ were grown on EMM agar minus uracil containing 6 mM hydroxyurea at 30°C for 5 days. (B) *cds1*$^+$ suppresses *rad26.a14* when S phase is arrested by *cdc22*. *rad26.a14 cdc22* double mutant independently transformed with pUR19 vector, pUR19-*rad26*$^+$, or pUR19-*cds1*$^+$ was first grown on EMM agar minus uracil at 25°C for 5 days. Cells were replica plated, incubated at 36°C for 12 h, and then shifted to 25°C to recover for 24 h. (C) *cds1*$^+$ does not suppress *rad26.a14* when S phase is arrested by *cdc20*. *rad26.a14 cdc20* double mutant cells transformed independently with pUR19 vector, pUR19-*rad26*$^+$, or pUR19-*cds1*$^+$ were grown on EMM agar minus uracil at 25°C for 5 days. Cells were then replica plated and incubated at 36°C for 48 h. (D) Phenotypes of *rad26.a14 cdc20* double mutant transformed with pUR-*rad26*$^+$ or pUR-*cds1*$^+$ at the restrictive temperature. *rad26.a14 cdc20* double mutant transformed with pUR-*rad26*$^+$ or pUR-*cds1*$^+$ genomic clone was incubated at 36°C for 6 h. Cells were stained with DAPI and calcofluor.

observed 15% abnormal nuclear morphology was not due to inappropriate mitotic entry. It is worth noting that although *cdc17* has been used to identify many potential DNA damage checkpoint genes (3), the *rad26.a14 cdc17* double mutant had >80% relative viability after 6 h at 36°C (Table 4 and Fig. 6C). These results indicate that the *rad26.a14* mutant is defective in monitoring S-phase progression, particularly in regard to early S phase, and does not have a major role in monitoring either prestart G_1, late S phase, or unligated DNA.

TABLE 4. *rad26.a14* monitors S-phase progression to prevent premature mitosis

cdc mutant background	Flow cytometry profile[a]	% abnormal nuclear morphology[b]	
		rad26.a14	*chk1*Δ
cdc10	G_1	<10	50
cdc22	G_1/S	40	20
cdc20	G_1/S	>80	>80
cdc21	Early S	>80	>80
polαts13	Early S	70	>80
cdc24	S	75	>80
polδts03	Late S	30	75
cdc27	Late S/G_2	15	>80
cdc17	Late S/G_2	15	>80
cdc25	G_2	0	ND

[a] DNA content was measured 4 h after shift to nonpermissive temperature.
[b] Percent abnormal nuclear morphology was measured 6 h after shift to nonpermissive temperature.

Strains with *chk1*Δ in *cdc20*, *cdc21*, *polαts13*, *cdc24*, *polδts03*, *cdc27*, or *cdc17* genetic backgrounds at 36°C had 75 to 80% of cells displaying mitotic catastrophe nuclear morphology (Table 4), indicating that defects in these genes required for S phase are sensed by *chk1*$^+$. These results also suggest that the checkpoint defect associated with *rad26.a14* is due to a failure to activate *chk1*$^+$.

DISCUSSION

Using a novel genetic approach, we have isolated a panel of fission yeast mutants that are defective in monitoring S-phase progression and in preventing premature mitosis. Here, we discuss the *aya14* mutant, which contains a novel mutant allele of a previously identified cell cycle checkpoint gene, *rad26*$^+$.

Rationale for using a semidisabled DNA polymerase δ to screen mutants defective in S-phase feedback control. Using hydroxyurea sensitivity to screen for cell cycle checkpoint mutants has resulted predominantly in mutants that are defective in both S-phase feedback control and DNA damage check-

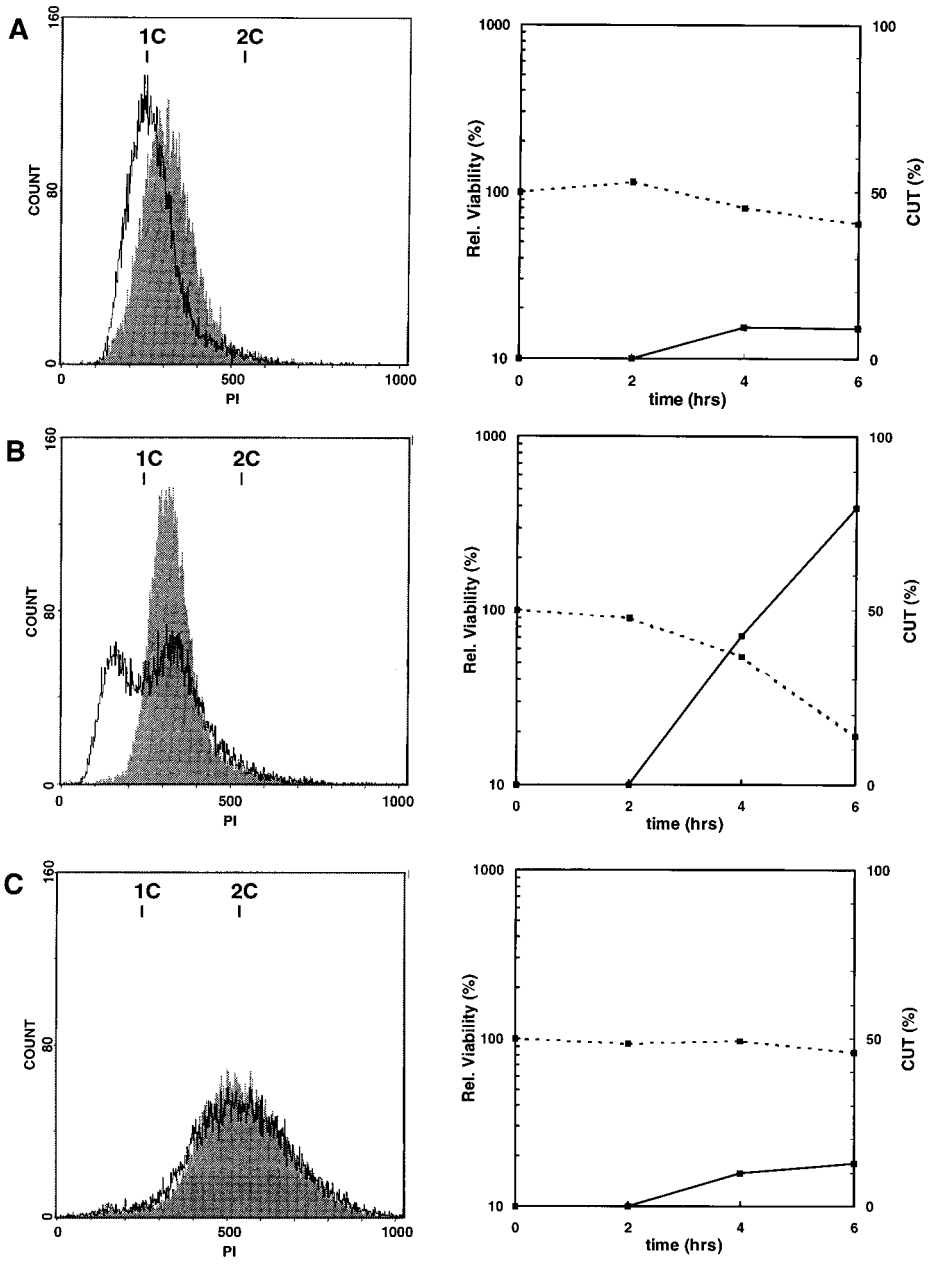

FIG. 6. The *rad26.a14* strain bypasses S-phase arrest but not cell cycle arrest at prestart G_1 or at late S/G_2. Cell cycle arrest profiles and relative viability data for *rad26.a14 cdc10* (A), *rad26.a14 cdc21* (B), and *rad26.a14 cdc17* (C) double mutants are shown. Flow cytometry analysis (left) shows cell cycle arrest DNA profiles in response to each *cdc* mutant after 6 h at 36°C. Shaded histograms represent the cell cycle arrest profiles of the background *cdc* mutants. Overlaid histograms represent the profiles of double mutants. 1C and 2C positions were defined by *cdc10* and *cdc25* mutants (arrested at 36°C for 4 h), respectively. Relative viability (broken line) and percentage of cells which underwent premature mitotic entry described as *cut* (solid line) are shown on the right for each double mutant panel. Cell viability was determined by plating uniform dilutions of cells at each time point onto rich medium and counting colonies after 5 days at 25°C. Percent cell viability was measured relative to cell samples taken immediately before the temperature shift. Since each *cdc* mutant has different viability kinetics after the temperature shift, the defect of *rad26.a14* at different stages of cell cycle arrest is shown as relative viability (rel. viability). Relative viability was calculated by dividing the percent cell viability of each double mutant by the percent cell viability of the respective background *cdc* mutant.

point (3, 4, 12). Since our goal was to identify mutants solely defective in S-phase feedback control, we used a semidisabled DNA polymerase δ to delay S phase instead of inhibiting S phase by hydroxyurea. The synthetic lethality of the *cdc2-3w pol*δ*ts03* double mutant at the semipermissive conditions (Table 2) clearly indicates that this approach is able to identify the S-M-phase checkpoint mutants. By this novel physiological approach, we identified a panel of mutants which is selectively deficient in the S-M-phase checkpoint control but not the DNA damage checkpoint (Table 3).

***aya14* is a novel mutant allele of *rad26*.** The original mutant allele of *rad26*, *rad26.T12*, was identified by using a hydroxyurea sensitivity screen (3). Interestingly, using a screen based on synthetic lethality with a semidisabled DNA polymerase δ, we isolated an *aya14* mutant which is allelic to *rad26*. *rad26.a14* differs from *rad26.T12* in many characteristics. In hydroxyurea,

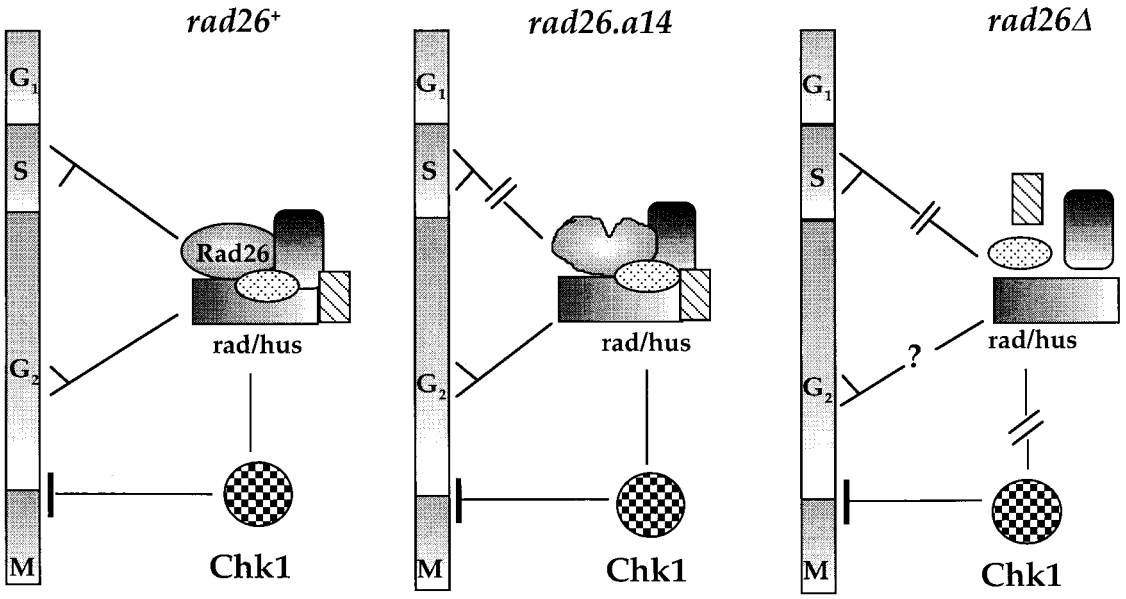

FIG. 7. A model for the role of the *rad26*$^+$ gene product, Rad26, in preventing mitosis during S-phase progression and in response to DNA damage at G_2/M-phase arrest. The proposed function of Rad26 in monitoring the order of cell cycle events is described in the Discussion section.

the *rad26.a14* strain has a higher percentage of cells displaying an abnormal nuclear phenotype than does the *rad26.T12* strain. Interestingly, the viability of *rad26.a14* cells is slightly higher than that of *rad26.T12* cells (data not shown). The radiation responses of these two alleles were also different (see Results). Furthermore, cells with the *rad26.T12* allele in a *pol*δ*ts03* genetic background die faster than the *rad26.a14 pol*δ*ts03* strain at the restrictive temperature (data not shown). However, both *rad26.T12* and *rad26.a14* cells are viable in the *wee1-50* genetic background (Fig. 3F [44a]). Data described in this study indicate that the *rad26.a14* mutant is defective in S-phase feedback control, while the *rad26.T12* mutant is defective in S-phase radiation response, suggesting a defect in a role related to DNA repair (3). These properties of *rad26*$^+$ are similar to those *rad1*$^+$ functions which can be separated into different groups by specific mutations (26).

Why does *cds1*$^+$ suppress the *rad26.a14* mutant's hydroxyurea sensitivity. *cds1*$^+$ has been proposed to generate the S-M-phase checkpoint via interaction with DNA polymerase α during S-phase progression (32). *cds1*$^+$ encodes a protein with a kinase motif which shares 35% amino acid identity with a *S. cerevisiae SPK1/SAD1/RAD53* protein (4, 51) and is indirectly involved in DNA-damage-induced transcription of the RNR large catalytic subunit, RNR2, and the free-radical-containing small subunit, RNR3 (4). The *cds1*$^+$ gene product may be similar to that encoded by *S. cerevisiae SAD1/RAD53*, being either directly or indirectly involved in the transcriptional induction of *cdc22*, which encodes the large catalytic subunit of RNR, or *suc22*, which encodes the small subunit of RNR (15). This could explain the *cds1*$^+$ suppression of the hydroxyurea sensitivity of the *rad26.a14* mutant, and its suppression of this mutant in a *cdc22* background but its inability to suppress the S-phase feedback control defect of the *rad26.a14* mutant when S phase is arrested by a defective DNA polymerase. Experiments are ongoing by us to test this possible role of *cds1*$^+$ (17a).

How does *rad26*$^+$ function in maintaining the dependency of cell cycle events. Results shown in Table 4 indicate that *chk1*$^+$, a key effector of the cell cycle checkpoint pathway (6, 46), can be activated by signals generated from different stages of the cell cycle arrest. *rad26.a14* is defective in the sensing of a signal(s) generated during S-phase progression, especially during early S-phase progression (Table 4 and Fig. 6), and has an intact DNA damage checkpoint (Fig. 3C and D). Finding that the *rad26.a14* strain is defective in mitotic arrest in early S phase could also explain the viability of the *rad26.a14 wee1-50* double mutant, since the function of *wee1*$^+$ is operative in late S and G_2 with a shortened G_2 (41). This property of the *rad26.a14* mutant is different from that of another S-M-phase checkpoint mutant, *rad1-S3*, which is not viable in a *cdc17* or a *wee1-50* background (26). This suggests that the signal sensed by *rad26.a14* is different from that sensed by *rad1.S3*. Together, these considerations suggest that there are different signals generated at different stages of the S phase. It is not yet known whether the signal is a DNA structure or a specific disrupted or stalled replication protein complex.

Two views of the possible function of the Rad26 protein provide support for different interpretations of our results. It has been proposed that the checkpoint *rad/hus* gene products form a "guardian complex" for maintaining both the S-M-phase checkpoint and the radiation checkpoint (3). In this protein complex, the *rad26*$^+$ gene product, Rad26, exists as a critical component to monitor the progression of S phase, while Rad1 functions as a docking protein (26) by interacting perhaps with Rad26 and/or other proteins in order to prevent premature mitosis. This complex monitors progression of S phase through Rad26, perhaps indirectly through Rad1, and monitors DNA damage by other sensors. However, both pathways require *chk1*$^+$ as the effector. Mutation at the *rad26.a14* allele results in a loss of ability of the complex to monitor the signal(s) generated during S-phase progression, especially the signal(s) generated during early S-phase progression, for the feedback control. This defect of the *rad26.a14* allele fails to activate *chk1*$^+$ during S-phase arrest, thus resulting in premature mitotic entry. This defect, however, does not cause an inability of the cell to activate *chk1*$^+$ and to arrest in G_2/M in response to DNA damage. Together, these findings suggest that *rad26*$^+$ may not be directly involved in sensing DNA

damage yet remains as a critical component of this cell cycle checkpoint pathway via interactions with other proteins that participate in the guardian complex. Deletion of *rad26*$^+$ (*rad26*Δ) causes either a complete disruption or the improper formation of the complex. Thus, *rad26*Δ cells lose the ability to activate *chk1*$^+$ and are therefore defective in both the G_2/M-phase radiation checkpoint and S-phase feedback control (Fig. 7).

Another possible view would be that cells require higher levels of functional complex to generate the S-M-phase checkpoint than the DNA damage checkpoint. If *rad26.a14* is a weaker allele compared to *rad26.T12* or *rad26*Δ, there may be a quantitative effect due to an insufficient level of *rad26.a14* which causes the observed defect in the S-M-phase checkpoint but not in the DNA damage checkpoint. We consider this hypothesis unlikely for the following reasons. (i) Another S-M-phase checkpoint *rad* mutant allele, *rad1-S3*, when expressed from a chromosomal locus, did not show any different effect on the S-M-phase checkpoint defect than that of *rad1-S3* expressed at multicopy levels (26). This finding strongly suggests that the S-M-phase checkpoint does not require higher levels of checkpoint gene function than the DNA damage checkpoint. (ii) The finding that *rad26.a14* is recessive further supports the notion that a single copy of the wild-type Rad26 is sufficient to compensate the Rad26.a14 mutant protein for the S-M-phase checkpoint function. (iii) A single incompletely replicated chromosome has an equal if not greater effect than that of a single DNA damage lesion on genome stability and cell viability. We therefore favor the guardian complex model shown in Fig. 7.

ACKNOWLEDGMENTS

We thank A. M. Carr for providing the *rad/hus* strains, S. Forsburg for most of the parental *cdc* strains, and P. Russell for the *wee1* mutant strain.

This work was supported by a grant from NIH (CA54415). I.G. is a postdoctoral fellow supported by the Swiss National Foundation, and D.J.F.G. is a postdoctoral fellow supported by the Wellcome International Prize Travel Research Fellowships (046754/Z/96/Z/JMW/LEC/CG).

REFERENCES

1. **Al-Khodairy, F., and A. M. Carr.** 1992. DNA repair mutants defining G2 checkpoint pathways in *Schizosaccharomyces pombe*. EMBO. J. **11:**1343–1350.
2. **Al-Khodairy, F., T. Enoch, I. M. Hagan, and A. M. Carr.** 1995. *Schizosaccharomyces pombe hus5* gene encodes a ubiquitin-conjugating enzyme required for normal mitosis. J. Cell Sci. **108:**475–486.
3. **Al-Khodairy, F., E. Fotou, K. S. Sheldrick, D. J. Griffiths, A. R. Lehmann, and A. M. Carr.** 1994. Identification and characterization of new elements involved in checkpoint and feedback controls in fission yeast. Mol. Biol. Cell **5:**147–160.
4. **Allen, J. B., Z. Zhou, W. Siede, E. C. Friedberg, and S. J. Elledge.** 1994. The *SAD/RAD53* protein kinase controls multiple checkpoints and DNA damage-induced transcription in yeast. Genes Dev. **8:**2416–2428.
5. **Barbet, N., W. J. Muriel, and A. M. Carr.** 1992. Versatile shuttle vectors and genomic libraries for use with *Schizosaccharomyces pombe*. Gene **114:**59–66.

5a. **Bhaumik, D., and T. S. Wang.** Unpublished data.

6. **Carr, A. M.** 1996. Checkpoints take the next step. Science **271:**314–315.
7. **Carr, A. M., and M. F. Hoekstra.** 1995. The cellular responses to DNA damage. Trends Cell Biol. **5:**32–40.
8. **Carr, A. M., M. Moudjou, N. J. Bentley, and I. M. Hagan.** 1995. The chk1 pathway is required to prevent mitosis following cell-cycle arrest at "start." Curr. Biol. **5:**1179–1190.
9. **D'Urso, G., B. Grallert, and P. Nurse.** 1995. DNA polymerase alpha, a component of the replication initiation complex, is essential for the checkpoint coupling S phase to mitosis in fission yeast. J. Cell Sci. **108:**3109–3118.
10. **Elledge, S. J.** 1996. Cell cycle checkpoints: preventing an identity crisis. Science **274:**1664–1672.
11. **Enoch, T., A. Carr, and P. Nurse.** 1993. Checkpoint check. Nature **361:**26.
12. **Enoch, T., A. M. Carr, and P. Nurse.** 1992. Fission yeast genes involved in coupling mitosis to completion of DNA replication. Genes Dev. **6:**2035–2046.
13. **Enoch, T., K. L. Gould, and P. Nurse.** 1991. Mitotic checkpoint control in fission yeast. Cold Spring Harbor Symp. Quant. Biol. **56:**409–416.
14. **Enoch, T., and P. Nurse.** 1990. Mutation of fission yeast cell cycle control genes abolishes dependence of mitosis on DNA replication. Cell **60:**665–673.
15. **Fernandez-Sarabia, M. J., C. McInerny, P. Harris, C. Gordon, and P. Fantes.** 1993. The cell cycle genes *cdc22* and *suc22* of fission yeast *Schizosaccharomyces pombe* encode the large and small subunits of ribonucleotide reductase. Mol. Gen. Genet. **238:**241–251.
16. **Francesconi, S., H. Park, and T. S. Wang.** 1993. Fission yeast with DNA polymerase δ temperature-sensitive alleles exhibits cell division cycle phenotype. Nucleic Acids Res. **21:**3821–3828.
17. **Griffiths, D. J. F., N. C. Barbet, S. McCready, A. R. Lehmann, and A. M. Carr.** 1995. Fission yeast *rad17*: a homologue of budding yeast *RAD24* that shares regions of sequence similarity with DNA polymerase accessory proteins. EMBO J. **14:**5812–5823.

17a. **Griffiths, D. J. F., et al.** Unpublished data.

18. **Gutz, H., H. Heslot, U. Leupold, and N. Loprieno.** 1974. *Schizosaccharomyces pombe*, p. 395–446. *In* R. C. King (ed.), Handbook of genetics 1, vol. I. Plenum Press, New York, N.Y.
19. **Hartwell, L. H., and T. A. Weinert.** 1989. Checkpoints: controls that ensure the order of cell cycle events. Science **246:**629–634.
20. **Hayles, J., and P. Nurse.** 1995. A pre-start checkpoint preventing mitosis in fission yeast acts independently of $p34^{cdc2}$ tyrosine phosphorylation. EMBO J. **14:**2760–2771.
21. **Hirano, T., S. Funahashi, T. Uemura, and M. Yanagida.** 1986. Isolation and characterization of *Schizosaccharomyces pombe* cut mutants that block nuclear division but not cytokinesis. EMBO J. **5:**2973–2979.
22. **Hoffman, C. S., and F. Winston.** 1987. A ten minutes DNA preparation from yeast efficiently releases autonomous plasmids for transformation of *Escherichia coli*. Gene **57:**267–272.
23. **Hofmann, J. X., and D. Beach.** 1994. cdt1 is an essential target of the *cdc10/Sct1* transcription factor: requirement for DNA replication and inhibition of mitosis. EMBO J. **13:**425–434.
24. **Humphrey, T., and T. Enoch.** 1995. Keeping mitosis in check. Curr. Biol. **5:**376–378.
25. **Jimenez, G., J. Yucel, R. Rowley, and S. Subramani.** 1992. The rad3+ gene of *Schizosaccharomyces pombe* is involved in multiple checkpoint functions and in DNA repair. Proc. Natl. Acad. Sci. USA **89:**4952–4956.
26. **Kanter-Smoler, G., K. E. Knudsen, G. Jimenez, P. Sunnerhagen, and S. Subramani.** 1995. Separation of phenotypes in mutant alleles of the *Schizosaccharomyces pombe* cell-cycle checkpoint gene *rad1*$^+$. Mol. Biol. Cell **6:**1793–1805.
27. **Kelly, T. J., G. S. Martin, S. L. Forsburg, R. J. Stephen, A. Russo, and P. Nurse.** 1993. The fission yeast *cdc18*$^+$ gene product couples S phase to START and mitosis. Cell **74:**371–382.
28. **Li, J. J., and R. J. Deshaies.** 1993. Exercising self-restraint: discouraging illicit acts of S and M in eukaryotes. Cell **74:**223–226.
29. **Lydall, D., and T. A. Weinert.** 1995. Yeast checkpoint genes in DNA damage processing: implications for repair and arrest. Science **270:**1488–1491.
30. **Maniatis, T., E. F. Fritsch, and J. Sambrook.** 1982. Molecular cloning: a laboratory manual. Cold Spring Harbor Laboratory, Cold Spring Harbor, N.Y.
31. **Moreno, S., A. Klar, and P. Nurse.** 1991. Molecular genetic analysis of fission yeast *Schizosaccharomyces pombe*. Methods Enzymol. **194:**795–823.
32. **Murakami, H., and H. Okayama.** 1995. A kinase from fission yeast responsible for blocking mitosis in S phase. Nature **374:**817–819.
33. **Murray, A. W.** 1992. Creative blocks: cell cycle checkpoints and feedback controls. Nature **359:**599–604.
34. **Nurse, P.** 1975. Genetic control of cell size at cell division in yeast. Nature **256:**547–551.
35. **Nurse, P.** 1994. Ordering S phase and M phase in the cell cycle. Cell **79:**547–550.
36. **Nurse, P., P. Thuriaux, and K. Nasmyth.** 1976. Genetic control of the cell division cycle in the fission yeast *Schizosaccharomyces pombe*. Mol. Gen. Genet. **146:**167–178.
37. **Paulovich, A. G., and L. H. Hartwell.** 1995. A checkpoint regulates the rate of progression through S phase in *S. cerevisiae* in response to DNA damage. Cell **82:**841–847.
38. **Paulovich, A. G., D. P. Toxzyski, and L. H. Hartwell.** 1997. When checkpoints fail. Cell **88:**315–321.
39. **Rowley, R.** 1992. Radiation-induced mitotic delay: a genetic characterization in the fission yeast. Radiat. Res. **132:**144–152.
40. **Rowley, R., S. Subramani, and P. G. Young.** 1992. Checkpoint controls in *Schizosaccharomyces pombe*: *rad1*. EMBO J. **11:**1335–1342.
41. **Russell, P., and P. Nurse.** 1987. Negative regulation of mitosis by *wee1*$^+$, a gene encoding a protein kinase homolog. Cell **49:**559–567.
42. **Saka, Y., and M. Yanagida.** 1993. Fission yeast *cut5*$^+$, required for S phase onset and M phase restraint, is identical to the radiation-damage repair gene rad4+. Cell **74:**383–393.
43. **Sazer, S., and S. W. Sherwood.** 1990. Mitochondrial growth and DNA synthesis occur in the absence of nuclear DNA replication in fission yeast. J. Cell Sci. **97:**509–516.

44. **Sheldrick, K. S., and A. M. Carr.** 1993. Feedback controls and G_2 checkpoints: fission yeast as a model system. Bioessays **15:**775–782.
44a. **Uchiyama, M.** Unpublished data.
45. **Walworth, N., S. Daveyk, and D. Beach.** 1993. Fission yeast chk1 protein kinase links the rad checkpoint pathway to cdc2. Nature **363:**368–371.
46. **Walworth, N. C., and R. Bernards.** 1996. rad-dependent response of the chk1-encoded protein kinase at the DNA damage checkpoint. Science **271:** 353–356.
47. **Wang, T. S.-F.** 1996. Cellular DNA polymerases, p. 461–493. *In* M. L. DePamphilis (ed.), DNA replication in eukaryotic cells. Cold Spring Harbor Laboratory Press, Cold Spring Harbor, N.Y.
48. **Weinert, T. A., and L. H. Hartwell.** 1993. Cell cycle arrest of cdc mutants and specificity of the *Rad9* checkpoint. Genetics **134:**63–80.
49. **Weinert, T. A., and L. H. Hartwell.** 1988. The *Rad9* gene controls the cell cycle response to DNA damage in *Saccharomyces cerevisiae*. Science **241:** 317–322.
50. **Weinert, T. A., G. L. Kiser, and L. H. Hartwell.** 1994. Mitotic checkpoint genes in budding yeast and the dependence of mitosis on DNA replication and repair. Genes Dev. **8:**652–665.
51. **Zheng, P., D. S. Fay, J. Burton, H. Xiao, J. L. Pinkham, and D. F. Stern.** 1993. *SPK1* is an essential S-phase-specific gene of *Saccharomyces cerevisiae* that encodes a nuclear serine/threonine/tyrosine kinase. Mol. Cell. Biol. **13:**5829–5842.